FUTURE e^+e^- LINEAR COLLIDERS AND BEAM-BEAM EFFECTS*

P. B. WILSON

Stanford Linear Accelerator Center, Stanford, California 94305

1. Introduction

As designers of the high energy accelerators of the future, the first question we must ask is, "What do the particle physicists want?" It is a fundamental fact of nature that the cross sections for the production of interesting events in electron-positron collisions in the TeV energy range tend to fall-off inversely as the square of the particle energy.[1] The luminosity for two colliding beams, either in a storage ring or from a linear collider, is defined as the event rate divided by the cross section. In order to keep the event rate at an acceptable level, the luminosity must therefore increase approximately as the square of the beam energy. In Table I the luminosities which follow this scaling are shown for four collider energies. The first row gives the energy and luminosity, at turn-on and after potential luminosity up-grades, for the Stanford Linear Collider (SLC). The next three rows give parameters for future and far future linear colliders. The machines that have been suggested for more detailed parametric studies in general fall into the three energy and luminosity categories shown in the table.

Table I. Present and Future High Energy Linear Colliders

Energy	Luminosity	Total Length (2 linacs) in km		
Per Linac	($cm^{-2}\,sec^{-1}$)	G=20 MV/m	G=200 MV/m	G=1 GV/m
50 GeV	$6 \times 10^{29-30}$	5	0.5	0.1
350 GeV	$\cdot 10^{32}$	35	3.5	0.7
1–1.5 TeV	10^{33}	100–150	10–15	2–3
5 TeV	10^{34}	500	50	10

Numerous concepts, ranging from conventional to highly exotic, have been proposed for the acceleration of electrons and positrons to very high energies. For any such concept to be viable, it must be possible to produce from it a set of consistent parameters for one of these "benchmark" machines. In this paper our attention will be directed to the choice of parameters for a collider in the 300 GeV energy range, operating at a gradient on the order of 200 MV/m, using X-band power souces to drive a conventional disk-loaded accelerating structure. These RF power sources, while not completely conventional, represent a reasonable extrapolation from present technology.

The choice of linac parameters is strongly coupled to various beam-beam effects which take place when the electron and positron bunches collide. We summarize these beam-beam effects in the next section, and then return to the RF design of a 650 GeV center-of-mass collider.

1. Summary of Beam Beam Effects

LUMINOSITY

The luminosity for the collision of two gaussian bunches is given by

$$\mathcal{L}_1 = N^2 f_r H_D / 4\pi A \quad , \qquad (2.1)$$

where N is the number of particles per bunch, f_r is the bunch collision rate, H_D is the pinch enhancement factor due to disruption (see next section) and $A = \sigma_x\sigma_y$ is the beam area. The area is in turn related to the normalized emittance $\epsilon_n = \epsilon_{nx} = \epsilon_{ny}$ by

$$A = \epsilon_n \left(\beta_x^*\beta_y^*\right)^{1/2} / \gamma \quad , \qquad (2.2)$$

where γ is the ratio of electron energy to rest energy and β_x^* and β_y^* are the beta functions at the collision point.

If a single bunch is accelerated during each linac pulse, then fr is also the linac repetition rate and the luminosity is the single bunch luminosity $\mathcal{L}_1$. The situation is more complex if, rather than single bunches, a train of b bunches is accelerated during each linac pulse. There are then several options for producing bunch collisions. Successive bunches can be switched to collide at different interaction points, as shown at (a) in Fig. 1. The luminosity summed over all interaction regions is then $\mathcal{L}_{sum} = b\mathcal{L}_1$. A second option is to collide bunches at an angle α, as shown at (b) in Fig. 1, where α is less than the transverse to longitudinal aspect ratio σ_x/σ_z. Only corresponding bunches in each of the two bunch train will collide. Noncorresponding bunches will miss each other, although if the collisions are highly disruptive bunches at the rear of the train will pass through debris from earlier collisions. For this option the total luminosity at the single interaction point is $\mathcal{L}_{tot} = b\mathcal{L}_1$. A third option is to collide a train of bunches head on as shown at (c) in Fig. 1. There are 2b-1 interaction points spaced a distance $\Delta s/2$ apart, where Δs is the bunch spacing. If the collisions are sufficiently nondisruptive, then the luminosity summed over all interaction point is $\mathcal{L}_{sum} = b^2\mathcal{L}_1$. The luminosity is different at each interaction point, the luminosity at the mth interaction point being given by

$$\mathcal{L}_m = \mathcal{L}_1 \times (1, 2, \ldots b-1, b, b-1, \ldots 2, 1) \quad .$$

If the collisions are highly disruptive, then the only effective collisions take place at the central interaction point, where $\mathcal{L}_{tot} = b\mathcal{L}_1$.

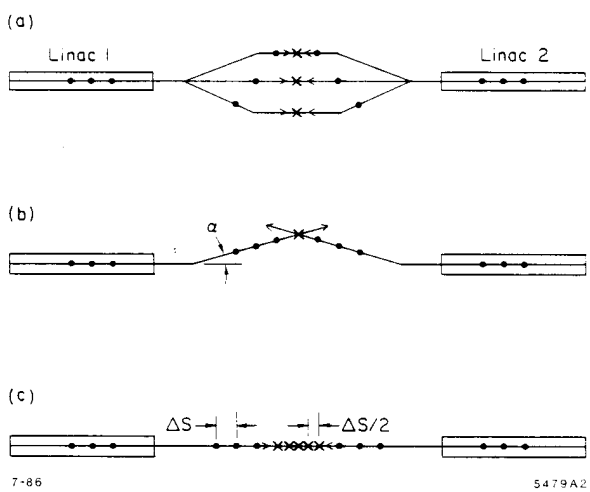

Fig. 1. Possible collision modes for bunch trains in a linear collider

*Work supported by the Department of Energy, contract DE-AC03-76SF00515.

DISRUPTION

When an electron bunch collides with a positron bunch, the collective field from the particles in one beam acts like a lens to focus the particles in the opposing beam toward the axis. For particles near the the axis in a gaussian bunch, the focal length of this lens is σ_z/D, where σ_z is the bunch length and D is the disruption parameter defined as

$$D = D_y = \frac{r_0 N \sigma_z}{\gamma A}\left(\frac{2R}{1+R}\right) \quad . \qquad (2.3)$$

Here $A = \sigma_x\sigma_y$, $R = \sigma_x/\sigma_y \geq 1$ is the aspect ratio and $r_0 = 2.82 \times 10^{-13}$ cm is the classical electron radius. If the disruption parameter is on the order of one the bunches pinch substantially as they pass through each other, reducing the effective transverse bunch area and enhancing the luminosity. The enhancement factor H_D has been computed from a simulation by R. Hollebeek,[2,3] and is shown in Fig. 2. For a flat beam ($R >> 1$) one would expect the pinch enhancement to vary approximately as the square root of the enhancement for a round beam, as shown by the dashed line in Fig. 2. Agreement with simulation results is seen to be reasonable. For intermediate values of R an approximate analytic expression for $H_D(R)$ in terms of $H_D\,(R = 1)$ is given in Ref. 4.

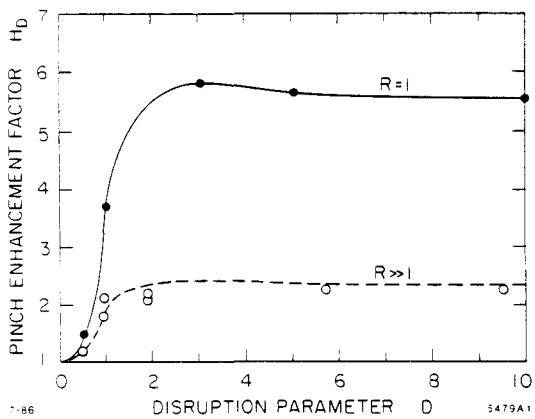

Fig. 2. Pinch enhancement factor as a function of disruption parameter for round and flat beams. Points shown are simulation results from Ref. 3.

BEAMSTRAHLUNG.

An electron or positron moving in the collective field of the oncoming beam emits synchrotron radiation, in this case called beamstrahlung. In classical synchrotron radiation, the power spectrum for the emission of photons of energy $\hbar\omega$ increases as $\omega^{1/3}$ for photons of low energy to a peak near the critical energy at $\hbar\omega_c = 3\hbar\gamma^2 eB/2mc$. Above the critical energy the spectrum falls off exponentially. By integrating the power spectrum over all frequencies, the total rate at which energy is radiated is obtained as $P \sim \gamma^2 B^2$. As either energy or magnetic field strength is increased, the critical energy will also increase until at some point $\hbar\omega_c$ exceeds γmc^2. One photon at the critical energy would then have to carry away more than the entire energy of the electron. A correct quantum calculation[5] shows, however, that the radiation spectrum is suppressed for $\hbar\omega > \gamma mc^2$, as shown in Fig. 3. The total radiated power is reduced by an amount corresponding to

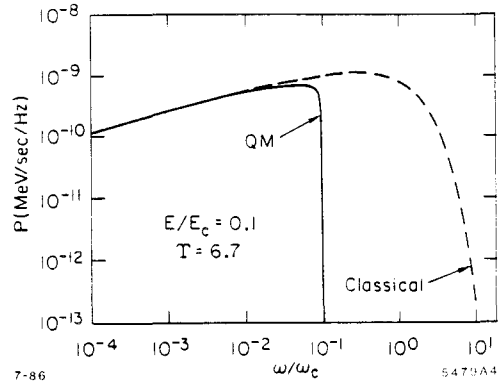

Fig. 3. Synchrotron radiation spectrum for a 5 TeV electron moving in a magnetic field of 30 MG. Dashed and solid lines show the difference between classical and quantum calculations.

the area between the solid and dashed lines. Define a scaling parameter Υ by

$$\Upsilon \equiv \frac{2\hbar\omega_c}{3\gamma mc^2} = \frac{\gamma B}{B_c} \quad , \qquad (2.4)$$

where $B_c = 4.4 \times 10^{13}$ G. In the classical regime ($\Upsilon << 1$) the total radiated power is proportional to $\Upsilon^2 \sim \gamma^2 B^2$, while for $\Upsilon >> 1$ the power is proportional to $\Upsilon^{2/3}$. In the quantum limit, the radiated power is reduced compared to the classical radiation rate by the factor $0.556\,\Upsilon^{-4/3}$. This reduction factor, H_Υ, is plotted as a function of Υ in Fig. 4.

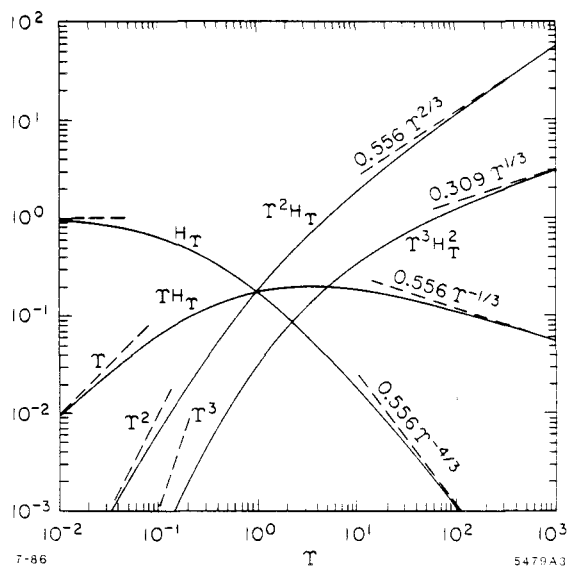

Fig. 4. Several useful functions of the quantum beamstrahlung parameter Υ

The preceeding discussion was valid for a single electron moving in a constant magnetic field. When two gaussian bunches collide, particles see a range of collective fields from zero on the axis to a maximum near one sigma in the transverse direction. Using the power spectrum for classical synchrotron radiation, Bassetti and Gygi-Hanney[6] have calculated the average energy loss per particle, divided by the incident energy, to be

$$\delta_{c\ell} = \frac{F_1 r_0^3 \gamma N^2}{\sigma_z A}\left[\frac{4R}{(1+R)^2}\right] , \qquad (2.5)$$

where $F_1 = 0.22$ is a form factor independent, to within a few percent, of the aspect ratio R.

It is expected that the radiation will be significantly reduced when single particle values for Υ at the position of maximum transverse field in the opposing bunch are on the order of one. In a breamstrahlung simulation, R. Noble[7] has shown that the reduction in energy loss per particle, averaged over the entire bunch, can be expressed by the single particle reduction factor H_Υ if an effective Υ, denoted by $\overline{\Upsilon}$, is defined in terms of the bunch parameters as

$$\overline{\Upsilon} = \frac{F_2 r_0 \lambda\!\!\!^{-}_c \gamma N}{\sigma_z A^{1/2}}\left[\frac{2R^{1/2}}{1+R}\right] H_D^{1/2} . \qquad (2.6)$$

Here $\lambda\!\!\!^{-}_c = 3.86 \times 10^{-11}$ is the Compton electron wavelength divided by 2π and $F_2 = 0.43$ is a form factor determined from the simulation. A factor $H_D^{1/2}$ is included to take pinch enhancement into account. Thus the beamstrahlung parameter for colliding gaussian bunches can be expressed as

$$\delta = \delta_{c\ell}\, H_D\, H_\Upsilon(\overline{\Upsilon}) , \qquad (2.7)$$

where again a factor H_D is included to take pinch into account.

CENTER-OF-MASS RMS ENERGY SPREAD

For particle physics, the center-of-mass rms energy spread, σ_W, is of more importance then the average energy loss per electron calculated after the bunches have collided. The relation between δ and σ_W/W for gaussian bunches depends[7] only on $\overline{\Upsilon}$. In the classical limit ($\overline{\Upsilon} \ll 1$) $\sigma_W/W = 0.32\,\delta$, while in the quantum limit ($\overline{\Upsilon} \gg 1$) $\sigma_W/W = 0.55\,\delta^{1/2}$. These contrasting limits on σ_W/W are a consequence of the strong variation in average number of photons, N_p, emitted per electron as a function of $\overline{\Upsilon}$. In the classical limit, $N_p = 2.1\,\delta/\overline{\Upsilon}$, while in the quantum limit $N_p = 3.9\,\delta$. Thus in the classical limit, $\sigma_W/W = 0.12$ for $\delta = 0.30$. For $\delta = 0.30$ in the quantum limit, however, $N_p = 1.1$ and $\sigma_W/W = 0.30$ (see Ref. 8).

SUMMARY AND COMBINED RELATIONS

From Eqs. (2.1), (2.5) and (2.6) we note that $\mathcal{L}_1$, $\delta_{c\ell}$ and $\overline{\Upsilon}$ all depend on N^2/A. This makes it possible to combine these parameters in various useful ways. In Table II the beam-beam parameters and some of these combinations are written in practical units. Of special importance are the functions $\overline{\Upsilon} H_\Upsilon \sim \delta(f_r/\mathcal{L}_1)^{1/2} \sim A^{1/2}\,\delta/N$ and $\overline{\Upsilon}^2 H_\Upsilon \sim E_0\delta/\sigma_z$. These function are plotted in Fig. 4. Also plotted is $\Upsilon^3 H_\Upsilon^2 \sim \delta^2/A^{1/2}D$.

A final beam parameter of interest is the beam power, $P_b = \gamma mc^2 N f_r$. In the practical units of Table II,

$$P_b(MW) = 1.6\times 10^{-3}\,\{N\,E_0\,b\,f_r\} , \qquad (2.16a)$$

$$= 21.7\left\{\frac{bE_0\mathcal{L}_1 A^{1/2}\overline{\Upsilon}H_\Upsilon}{H_D^{1/2}\,\delta}\right\}\left[\frac{2R^{1/2}}{1+R}\right] . \qquad (2.16b)$$

Table II. Beam–Beam Expressions in Practical Units

E_0 (TeV)	σ_z (mm)	N (10^{10})
$\mathcal{L}_1(10^{32}/\mathrm{cm}^2/\mathrm{sec})$	A (μm)^2	f_r (Hz)

$$\mathcal{L}_1 = 8.0\times 10^{-6}\left\{\frac{N^2 f_r H_D}{A}\right\} \qquad (2.8)$$

$$D = 1.44\times 10^{-2}\left\{\frac{N\sigma_z}{E_0 A}\right\}\left[\frac{2R}{1+R}\right] \qquad (2.9)$$

$$\delta = 9.9\times 10^{-4}\left\{\frac{N^2 E_0 H_D H_\Upsilon}{\sigma_z A}\right\}\left[\frac{4R}{(1+R)^2}\right] \qquad (2.10)$$

$$\overline{\Upsilon} = 9.2\times 10^{-3}\left\{\frac{N E_0 H_D^{1/2}}{\sigma_z A^{1/2}}\right\}\left[\frac{2R^{1/2}}{1+R}\right] \qquad (2.11a)$$

$$= 3.27\left\{\frac{E_0\mathcal{L}_1^{1/2}}{\sigma_z f_r^{1/2}}\right\}\left[\frac{2R^{1/2}}{1+R}\right] \qquad (2.11b)$$

$$\overline{\Upsilon} H_\Upsilon = 2.6\times 10^{-2}\left\{\frac{f_r^{1/2}\delta}{\mathcal{L}_1^{1/2}}\right\}\left[\frac{1+R}{2R^{1/2}}\right] \qquad (2.12)$$

$$\overline{\Upsilon}^2 H_\Upsilon = 8.5\times 10^{-2}\left\{\frac{E_0\delta}{\sigma_z}\right\} \qquad (2.13)$$

$$N = 9.2\left\{\frac{A^{1/2}\delta}{H_D^{1/2}\overline{\Upsilon}H_\Upsilon}\right\}\left[\frac{1+R}{2R^{1/2}}\right] \qquad (2.14)$$

$$DH_D^{1/2} = 1.13\times 10^{-2}\left\{\frac{\delta^2}{\overline{\Upsilon}^3 H_\Upsilon^2 A^{1/2}}\right\}\left[R^{1/2}\right] \qquad (2.15)$$

3. RF and Structure Parameters

Energy in an electromagnetic field delivered to some sort of structure is required to accelerate charged particles. The structure can be a metallic waveguide, such as the traditional disk-loaded accelerator structure, an open resonator, a wake-field "transformer," or in a general sense even a plasma. Also required is a driver to convert power from the AC line into the electromagnetic energy delivered to the structure. The driver can be a microwave tube, a laser, or a driving bunch as in the wake field accelerator. A conceptual diagram of a generalized driver and accelerating structure is shown in Fig. 5.

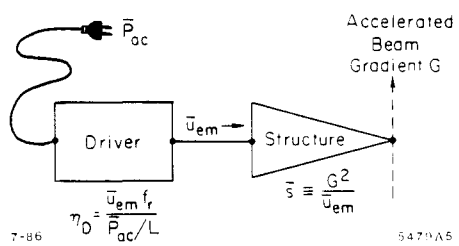

Fig. 5. Conceptual diagram of an accelerator.

A figure of merit for the accelerating structure is the efficiency with which it converts average input electromagnetic energy per unit length, u_{em}, into average accelerating gradient G. The dimension of G^2/u_{em} is that of an inverse capacitance, or elastance, per unit length.[9] A figure of merit for the driver is the efficiency with which it converts wall plug energy into electromagnetic energy delivered to the structure. In this paper we focus on the case of a conventional linac in which the driver is a microwave tube (plus pulse compression) and the structure

is a conventional disk-loaded structure. The parameters η_D and $\bar{s}$ are, however, more generally useful for comparing the various exotic and conventional acceleration schemes that have been proposed for high energy colliders.

Consider a SLAC-type $2\pi/3$-mode disk-loaded traveling wave structure. As the beam aperture radius a is increased, we find that the group velocity v_g increases approximately as a^4, and the elastance $s \equiv G^2/u$, where u is the stored energy per unit length, decreases. The unloaded Q, on the other hand, is approximately independent of the beam aperture radius. Thus

$$a/\lambda \approx 8.42 \times 10^{-2} \left[v_g(m/\mu s)\right]^{1/4} \qquad (3.1)$$

$$s\left(\frac{\Omega}{ps-m}\right) \approx \frac{13.24\,[f(GHz)]^2}{1+0.216\,[v_g(m/\mu s)]^{1/2}} \qquad (3.2)$$

$$T_0(\mu s) \equiv \frac{2Q_0}{\omega} \approx 7.1\,[f(GHz)]^{-3/2} \quad . \qquad (3.3)$$

The above relations are strictly valid only for constant impedance (constant beam aperture) structures. For a constant gradient structure, in which the beam aperture decreases along the structure in order to maintain a constant accelerating field, the situation is more complex. However, if the attenuation parameter (defined by $\tau \equiv T_f/T_0$ where T_f is the filling time) is not too large, then an effective group velocity $\bar{v}_g \equiv L_s/T_f$ can be used in the above expressions to give approximate average values for the structure. The smallest beam aperture at the end of the structure will then be less than that given by Eq. (3.1) by a factor $e^{-\tau/4}$.

Because of losses (and the spatial variation in the accelerating field in the case of a constant impedance structure), the effective stored energy in the structure at the end of the filling time is less than the input energy by the structure efficiency factor η_s. For a constant gradient structure

$$\eta_s = \frac{1-e^{-2\tau}}{2\tau} \quad . \qquad (3.4)$$

Note that structure figure of merit, as defined in Fig. 5, is $\bar{s} = s\eta_s$. The peak input power to the structure is now

$$\hat{P}_s = \frac{G^2 L_s}{\eta_s T_f s} \quad . \qquad (3.5)$$

RF pulse compression can be used to reduce the required peak power using the binary power multiplication (BPM) scheme of Z. D. Farkas.[10] The peak power gain for an n-stage BPM is

$$M = 2^n \eta_c \quad , \qquad (3.6)$$

where η_c is the compression efficiency given by

$$\eta_c = 2^{-n}\left\{[1+\exp(-2\alpha T_f)]\right.$$
$$\left.[1+\exp(-4\alpha T_f)]\ \ldots\ [1+\exp(-2^n\alpha T_f)]\right\} \quad .$$

Here α is the delay line attenuation per unit time. If each RF source feeds N_s accelerating structures, then the peak source power will be

$$\hat{P}_k = \frac{N_s L_s G^2}{M \eta_s T_f s} \quad . \qquad (3.8)$$

The average source power will be $\overline{P}_k = 2^n T_f f_r \hat{P}_k$, and the total AC "wall plug" power per linac of length L is

$$\overline{P}_{ac} = \frac{N_k \overline{P}_k}{\eta_{rf}} = \frac{f_r L G^2}{\eta_{rf}\eta_c\eta_s s} = \frac{f_r L G^2}{\eta_D \bar{s}} \quad . \qquad (3.9)$$

Here $N_k = L/N_s L_s$ is the total number of RF sources per linac, η_{rf} is the efficiency for the conversion of wall plug power to RF power, $\eta_D = \eta_{rf}\eta_c$ is the overall driver efficiency and $\bar{s} = s\eta_s$ is the net structure elastance. It is also useful to know the average power dissipation per unit length of accelerating structure, given by (constant gradient case)

$$\frac{\overline{P}_{diss}}{L_s} = \frac{2\tau f_r G^2}{s} \quad . \qquad (3.10)$$

As a design example, consider two X-band linacs (f = 11.4 GHz) driven by microwave tubes, each with a peak output power of 150 MW and a pulse length of 1.8 μs. Let each accelerating structure be 1.0 m in length, assume four stages of pulse compression, and let each RF source feed four accelerating sections. Thus the filling time is $T_f = 1.8\,\mu s/16 = .112\,\mu s$, and the other structure parameters given in Table III follow. If the attenuation of the delay lines in the pulse compression system is $\alpha = 0.10$ nepers per microsecond (3 in I.D. overmoded copper pipe), then the compression efficiency is $\eta_c = 0.85$, the peak power multiplication factor is M = 13.6, and the gradient G = 186 MV/m follows from Eq. (3.8). The energy of each linac is then 325 GeV. If we assume a repetition rate of 120 Hz and an efficiency $\eta_{rf} = 0.55$ for conversion of AC power to RF power, then the total wall plug power for both linacs is 50 MW. The RF source parameters are also summarized in Table III.

TABLE III. RF and Structure Parameters for a 325 + 325 GeV Linear Collider

STRUCTURE PARAMETERS		
Length per Linac L	1.75	km
Length Each Section L_s	1.0	m
Frequency f_{rf}	11.4	GHz
Filling Time T_f	112	ns
Internal Time Constant T_0	184	ns
Attenuation Parameter τ	0.61	
Average Group Velocity $\bar{v}_g$	8.9	m/μs
$\bar{v}_g / c$	0.0296	
Structure Efficiency η_s	0.58	
Internal Elastance s	1050	V/pC-m
Effective Elastance $\bar{s}$	610	V/pC-m
Disk Hole Radius a	3.82	mm
RF SOURCE PARAMETERS		
Source Spacing $N_s L_s$	4.0	m
Total Number of Sources	438	/linac
Peak Source Power $\hat{P}_k$	150	MW
Pulse Length T_k	1.8	μs
Repetition Rate f_r	120	Hz
Average Source Power $\overline{P}_k$	32	kW
Pulse Compression Efficiency η_c	0.85	
Structure Average Power Dissipation	4.8	kW/m
Assumed RF efficiency η_{rf}	0.55	
Wall Plug Power $\overline{P}_{ac}$	25	MW/linac
Net Driver Efficiency η_D	0.47	

4. Beam–Structure Parameters

Several important collider parameters depend upon the interaction between the beam and the accelerating structure. The single bunch efficiency η_b, is important because it is a rough measure of the energy spread within the bunch produced by longitudinal wake fields. Also, the bunch-to-bunch energy droop between bunches in a bunch train is $\Delta E/E \approx \frac{1}{2}\eta_b$. The single bunch efficiency is

$$\eta_b = \frac{eNG}{u} = \frac{eNs}{G} = 1.6\times 10^{-3}\left\{\frac{N(10^{10})\, s(10^{12}\ \mathrm{V/C\text{-}m})}{G\ (\mathrm{MV/m})}\right\} \quad . \tag{4.1}$$

The single bunch energy spread can only be obtained exactly by a calculation using the longitudinal delta-function wake potential for the accelerating structure in question, as is explained in Ref. 11. For a short bunch sitting on the crest of the accelerating wave, the energy spread is given roughly by $(\Delta E/E)_{sb} \approx \frac{1}{2}B(\sigma_z)\eta_b$, where B is an enhancement factor taking into account the effect of higher-order longitudinal modes (see Ref. 11). For example, $B \approx 3$ for a 1 mm bunch in the SLAC structure. However, this energy spread can be reduced by adjusting the relative phase of the bunch with respect to the crest of the accelerating wave, such that the slope of the RF wave tends to compensate for the slope of the wake potential within the bunch. In this way the energy spread can be reduced by at least a factor of 3. A conservative estimate is then $(\Delta E/E)_{sb} < \eta_b/2$.

In order to obtain a high luminosity with a reasonable repetition rate and number of particles per bunch, a very small transverse emittance will be required. Significant growth in emittance as the bunch travels through the linac can lead to an unacceptable degradation in luminosity. A number of effects can produce such an emittance growth, but there is space here to focus on just one representative effect. The quadrupoles in the focusing lattice of the linac will jitter randomly in transverse position due to high frequency components in ground motion arising from both natural and man-made causes. The excursions off-axis by the head of the bunch will produce a transverse wake which wiggles the tail of the bunch. The growth in transverse beam size is given by[12]

$$\frac{\Delta x}{\sigma_f} = \frac{\sqrt{2}\, r_0\, N\, W_\perp\, \gamma\, d_{rms}}{\pi^{3/2}\, \epsilon_n^{1/2} (d\gamma/dz)^{3/2}} \quad . \tag{4.2}$$

Here $W_\perp$ is the transverse wake potential in cgs units (cm^{-3}), d_{rms} is the *rms* jitter amplitude, and σ_f is the bunch size at the end of the linac. For short bunches the transverse wake can be estimated from $W_\perp = 2\sigma_z W'_\perp$, where $W'_\perp$ is the slope of the delta function transverse wake potential. For the SLAC structure (λ = 10.5 cm, a = 1.165 cm), this slope is $W'_\perp = 2.1\ \mathrm{cm}^{-4}$ and scales as

$$W'_\perp \sim \omega^4\ (a/\lambda)^{-3.5} \quad . \tag{4.3}$$

The emitance growth due to magnet jitter can be reduced substantially by introducing an energy spread between the head and the tail of the bunch (Landau damping)[13]. However, Eq. (4.2) provides a measure of the severity of transverse wake field effects and is useful for scaling.

5. A 325 GeV Collider Example

Although it may seem like the backward way to do it, the RF parameters for our example collider were calculated first in Sec. 3 before the beam-beam parameters were considered. The RF frequency was chosen *a priori*, and the peak source power and pulse length were chosen to give the gradient necessary to reach 300$^+$ GeV in a linac 1.75 km in length. The repetition rate was fixed at 120 Hz to give a reasonable AC wall plug power. The energy and repetition rate, together with a luminosity per bunch of $10^{32}/\mathrm{cm}^2/\mathrm{sec}$ and a beamstrahlung parameter $\delta = 0.3$, fix $\Upsilon = 0.16$ and $\sigma_z = 0.6$ mm from Eqs. (2.12) and (2.13). The logical next step would be to fix η_b at a reasonable value of 1-2%, determine N through Eq. (4.1) and then A and hence ϵ_n from Eq. (2.14). We instead fix ϵ_n at 3×10^{-6} m-rad (one-tenth the SLC damping ring emittance), choose $\beta^* = 1$ mm, find $A^{1/2} = 0.07\ \mu$m and show that N, D and η_b are reasonable. From Eq. (2.15) and Fig. 2 we find D = 5.4, $H_D = 5.6$. From Eq. (2.14) it follows that $N = 9.4\times 10^9$, and from Eq. (4.1) $\eta_b = 0.85\%$. These results are summarized in Table IV. Following a similar procedure for a flat beam with $R = 10$, we obtain the results shown in the second row of Table IV. The last column gives σ_W/W obtained from data in Ref. 7.

Transverse emittance growth was checked by inserting these parameters in Eq. (4.2). The result is $\Delta x/\sigma_f \approx 0.06$ for the round beam case assuming $d_{rms} = 10^{-2}\ \mu$m. The high gradient and larger than normal disk hole radius help to keep emittance growth tolerable.

Table IV. Beam–Beam Parameters for Collider Example

E_0=325 GeV $\quad f_r = 120$ Hz $\quad \mathcal{L}_1 = 10^{32}/\mathrm{cm}^2/\mathrm{sec}$

$\delta = 0.3 \quad \epsilon_n = 3\times 10^{-6}$ m $\quad (\sigma_x^*\sigma_y^*)^{1/2} = 0.07\ \mu$m

R	$\bar{\Upsilon}$	H_Υ	σ_z (mm)	D	H_D	$N\,(10^{10})$	P_b (kW)	η_b (%)	σ_W/W
1	0.16	0.55	0.61	5.4	5.6	0.94	59	0.84	0.14
10	0.49	0.30	0.12	2.9	2.4	1.43	89	1.3	0.18

6. Some Conclusions

For the next generation of linear collider ($E_0 \geq 300GeV$), there is an advantage in working at a higher gradient than the SLC gradient of 20 MV/m in order to keep the total length of accelerating structure within reasonable bounds. In the preceding sections we have developed the design of a collider with a gradient on the order of 200 MV/m using conventional RF technology at 11 GHz (although some might argue that X-band microwave tubes delivering 150 MW are far from conventional). The same technology could be extended to build a 1 TeV collider with a luminosity of $10^{33}cm^{-2}sec^{-1}$, with a wall plug power on the order of 100 MW, if we can learn how to collide a train of 10 or 20 bunches spaced several nanoseconds apart. In the case of a 5 TeV collider, the machine becomes uncomfortably long even with a gradient of 200 MV/m (see Table I), and the wall plug power would approach the GW range. A higher RF frequency with a nonconventional RF power source (*e.g.*, two beam accelerator) may be required, or perhaps such a machine will be based on a completely different acceleration technology derived from one of the many exotic concepts that have been proposed.[14]

References and Notes

1. B. Richter in *Laser Acceleration of Particles, Malibu, CA, 1985,* C. Joshi and T. Katsouleas, eds., AIP Conf. Proc. **No. 130**, (Am. Inst. Phys., New York, 1985), pp.8–22.
2. R. Hollebeek, *Nucl. Instrum. Methods* **184**, 333 (1981).
3. R. Hollebeek and A. Minten, SLAC Internal Note CN–302 (1985).
4. P. Wilson in *Laser Acceleration of Particles, Malibu, CA, 1985,* C. Joshi and T. Katsouleas, eds., AIP Conf. Proc. **No. 130**, (Am. Inst. Phys., New York, 1985), p.562.
5. See for example T. Erber *et al., Proc. 12th Int. Conf. on High Energy Accelerators, Fermilab, August 1983,* p.372; also Thomas Erber, *Rev. Mod. Phys.* **38**, 626 (1966).
6. M. Bassetti and M. Gygi–Hanney, LEP–Note–221, CERN, Geneva (1980).
7. Robert J. Noble, SLAC–PUB–3871 (1986). See also K. Yokoya, KEK Preprint 85–53 (October 1985, also submitted to Nucl. Instrum. Methods), for an analytic calculation of beamstrahlung in the quantum regime.
8. For $N_p \approx 1$ higher moments in the electron energy distribution became comparable with σ_W, and this parameter is then of dubious usefulness.
9. The use of elastance for the ratio G^2/u was suggested by Z. D. Farkas. See *IEEE Trans. Nucl. Sci.* **NS-32**, No. 5, 3225 (1985).
10. Z. D. Farkas, *MTT Special Transactions Issue on New and Future Applications of Microwave Systems,* to be published in October 1986. Also SLAC–PUB–3662.
11. See for example P. B. Wilson in *Physics of High Energy Accelerators,* F. R. Huson and M. Month, eds., AIP Conf. Proc. **No. 87**, (Am. Inst. Phys., New York, 1982), Secs. 10.2 and 12.3; also SLAC–PUB–2884.
12. A. Chao and R. Ruth, private communication.
13. See for example K. L. F. Bane, *IEEE Trans. Nucl. Sci.* **NS–32**, No. 5, 2389 (1985); also SLAC–PUB–3670.
14. For a review of proposed acceleration concepts see articles in *Laser Acceleration of Particles, Malibu, CA, 1985,* C. Joshi and T. Katsouleas, eds., AIP Conf. Proc. **No. 130**, (Am. Inst. Phys., New York, 1985).